CR-123961

WYLE LABORATORIES

EASTERN OPERATIONS — HUNTSVILLE FACILITY

research report

26p

WYLE LABORATORIES - RESEARCH STAFF

REPORT WR 72-12

SHOCK WAVE OSCILLATION DRIVEN BY
TURBULENT BOUNDARY LAYER FLUCTUATIONS

By

Kenneth J. Plotkin

September 1972

WYLE LABORATORIES
EASTERN OPERATIONS, HUNTSVILLE, ALABAMA

i

ABSTRACT

Pressure fluctuations due to the interaction of a shock wave with a turbulent boundary layer are investigated. A simple model is proposed in which the shock wave is convected from its mean position by velocity fluctuations in the turbulent boundary layer. Displacement of the shock is assumed limited by a linear restoring mechanism. Predictions of peak root mean square pressure fluctuation and spectral density are in excellent agreement with available experimental data.

TABLE OF CONTENTS

LIST OF FIGURES

LIST OF SYMBOLS

a	=	Sound speed
D	=	Diameter of protuberance; diameter of axisymmetric model
f	=	Frequency
h	=	Height of step or protuberance
M	=	Mach number
p	=	Fluctuating pressure
P	=	Mean static pressure
q	=	Dynamic pressure
R	=	Correlation function
t	=	Time
u	=	Velocity
x	=	Displacement of shock wave from mean location
$\bar{x}$	=	Streamwise coordinate
β	=	See Equation (2)
δ	=	Boundary layer thickness
ϵ	=	Root mean square turbulent Mach number
$\mu(t)$	=	Random function representing turbulent velocity in boundary layer
ξ	=	Variable of integration
ρ	=	Density
τ	=	Time separation
τ_μ, τ_x	=	Integral scale; $\tau_i = \int_0^\infty R_i(\tau)\, d\tau$
ϕ	=	Spectral density

Subscripts

0	=	Condition just ahead of shock wave
T	=	Turbulent quantity
∞	=	Free-stream condition

Other Symbol

$\langle\ \rangle$	Ensemble average

1.0 INTRODUCTION

An important source of surface pressure fluctuations on high speed aerodynamic vehicles is the oscillation of shock waves. Figure 1 shows the static and fluctuating pressure levels associated with supersonic flow ahead of a flare or a three-dimensional protuberance. Other basic flow geometries containing oscillating shock waves exist, such as oscillation of a near normal terminal shock in transonic flow. Reference 1 provides detailed descriptions of fluctuating flow fields, and contains a comprehensive review of available experimental data. The flow field of Figure 1 will be briefly described here to provide a framework for the shock oscillation model presented in the next section.

There are three basic sources of fluctuating pressure in the flow field shown in Figure 1: the attached turbulent boundary layer ahead of the shock; the separated region behind the shock; and the oscillation of the shock itself. Figure 2 shows spectra of pressure fluctuations in these three parts of the flow field ahead of a 45° wedge, from Reference 2. Robertson (Reference 1) has pointed out that the spectrum at the shock location represents the spectrum associated with an oscillating shock wave alone, plus some fraction of the attached and detached spectra, as these two environments alternately appear at the mean shock location as the shock oscillates. Fluctuations from the attached boundary layer are much smaller than from separated flow and may be neglected, so the spectrum of fluctuations at the mean shock location is given by shock oscillation and separated flow environments. In Figure 2, the spectral shape follows the separated flow spectrum for $f \delta_0 / u_0 > 0.2$; the spectrum for shock oscillation alone would follow the dashed extrapolation.

Much of the analytical work on oscillating shock waves has followed the approach used by Trilling (Reference 3) for interaction of a shock wave with a laminar boundary layer. In that analysis, a harmonic perturbation to the mean flow was assumed, and it was shown that oscillation could be self-sustaining for certain frequencies. This approach is felt to be unsatisfactory to the present problem for two reasons. First, the source of the initial disturbance is not identified. In the experimental investigation of Reference 4, a spark discharge was used to artificially stimulate oscillation. Second, Trilling's analysis would lead us to expect dominant frequencies in the spectrum. The spectrum of Figure 2 does not contain any such peaks.
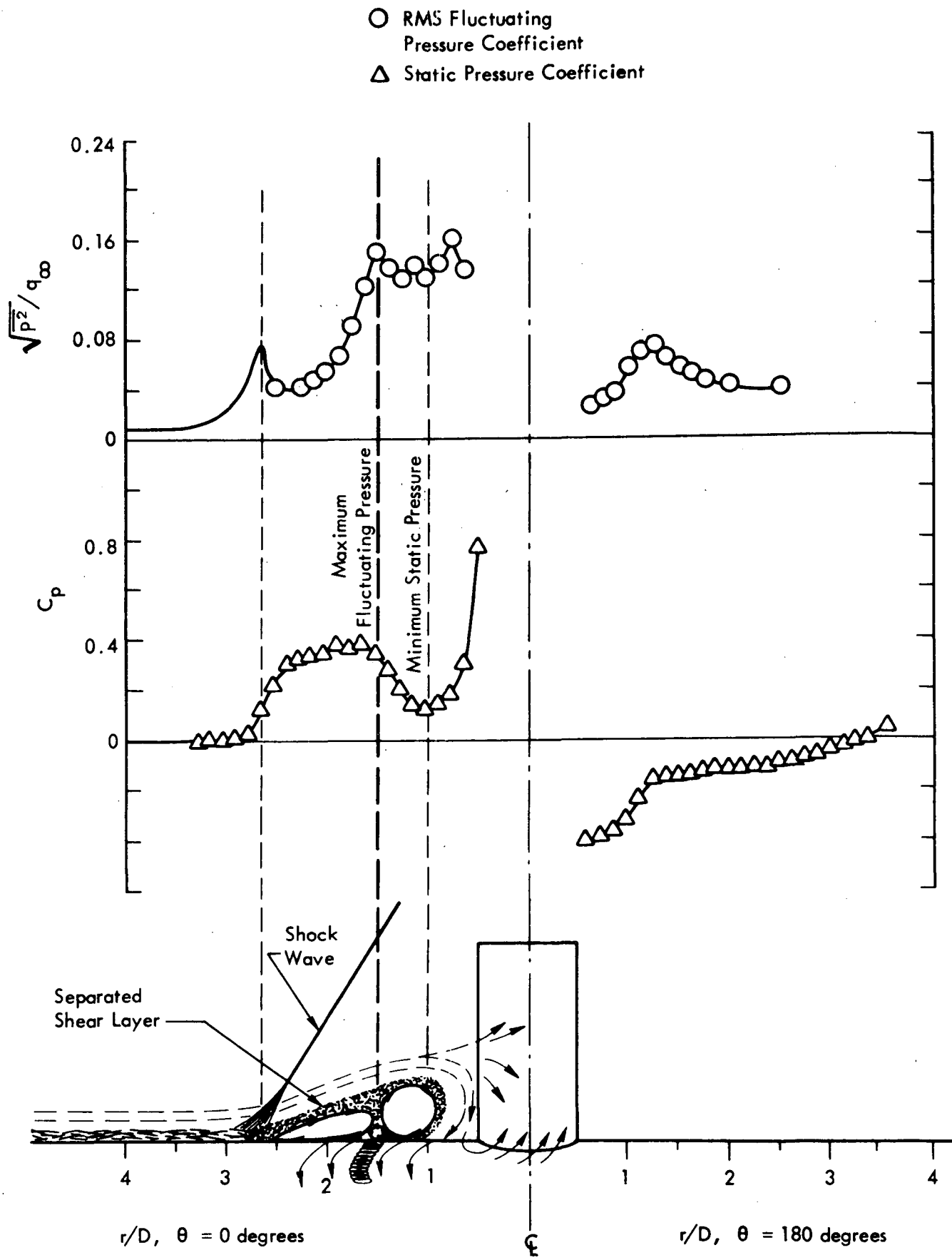
1

Figure 1. Composite Schematic of Protuberance Flow Field Characteristics, $M_\infty = 1.60$, h/D = 2.0, from Reference 1
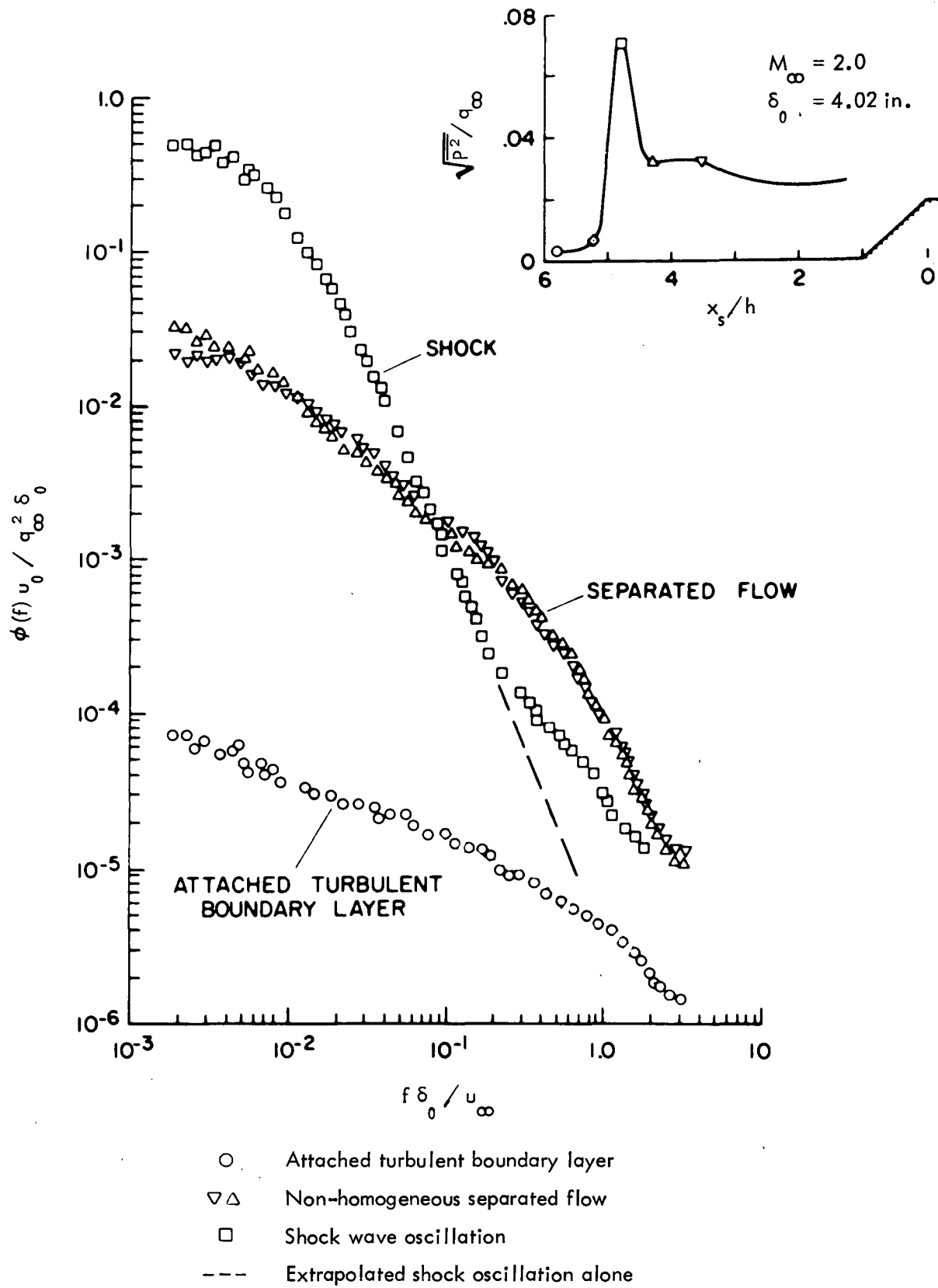
2

Figure 2. Longitudinal Distribution of Pressure Fluctuations and Typical
Power Spectra in Vicinity of Supersonic Flow Separation
Ahead of a 45° Wedge, from Reference 2

3

The broad band nature of observed shock oscillation spectra in the presence of a turbulent boundary layer suggests the following model. The mean location of the shock is a stable position, governed by mean flow conditions. (If this were not so, the shock would not be there.) As each turbulent eddy passes, the shock is convected upstream or downstream. The stability of the mean shock location causes a limit to the excursion distance. In the next section, an equation of motion for shock location is postulated, based on convective displacement and a linear restoring mechanism. Statistical properties of the shock motion are found from which mean square pressure fluctuations and spectra are calculated.

2.0 ANALYSIS

2.1 Equation of Motion of the Shock Wave

Velocity fluctuations in the x-direction (parallel to the wall) at a fixed point within the boundary layer may be represented as

$$u_{T_x} = a_\infty \, \epsilon \, \mu(t) \tag{1}$$

where $\mu(t)$ is a random function of time with $\langle \mu^2 \rangle = 1$, and ϵ is the turbulent Mach number $\langle u_{T_x}^2 \rangle^{\frac{1}{2}} / a_\infty$. A one-dimensional model is adopted, neglecting velocity fluctuations in other directions. The shock wave within the boundary layer is then convected in the x-direction with speed u_{T_x}.

After the shock wave is displaced a distance x (x small compared to scale length of the flow geometry), the flow geometry will be disturbed by an amount proportional to x. This in turn will disturb the pressure field by an amount proportional to x. The shock wave will then move with velocity proportional to x. Since the shock will move back toward its original position, this restoring velocity is given by

$$u_{restoring} = -\beta x \tag{2}$$

where β is a constant depending on the flow geometry. This constant will be deduced as the analysis proceeds.

The net speed of the shock wave is the sum of Equations (1) and (2):

$$u = a_\infty \, \epsilon \, \mu(t) - \beta x \tag{3}$$

The equation for the shock location is

5

$$\frac{dx}{dt} + \beta x = \epsilon \, a_\infty \, \mu(t) \tag{4}$$

Equation (4) may be integrated to give

$$x = e^{-\beta t} \, \epsilon \, a_\infty \int_0^t \mu(\xi) \, e^{\beta \xi} \, d\xi \tag{5}$$

In the following subsections, various statistical properties of x are calculated, leading to predictions of the intensity and spectral distribution of pressure fluctuations.

2.1.1 <u>Mean Square Shock Displacement</u> — Squaring Equation (5) and taking the ensemble average,

$$\langle x^2 \rangle = \epsilon^2 a_\infty^2 \, e^{-2\beta} \int_0^t \int_0^t \langle \mu(\xi_1) \mu(\xi_2) \rangle \, e^{\beta(\xi_1 + \xi_2)} \, d\xi_1 \, d\xi_2 \tag{6}$$

Changing integration variables from $\{\xi_1 , \xi_2\}$ to center of mass and relative coordinates $\{(\xi_1 + \xi_2)/2 , \xi_2 - \xi_1\}$, it is straightforward to obtain the following equation for $t \gg \tau_\mu$:

$$\langle x^2 \rangle = \epsilon^2 a_\infty^2 \, \frac{\tau_\mu}{\beta} \, (1 - e^{-\beta t}) \tag{7}$$

where:

$$\tau_\mu = \int_0^\infty R_\mu(t) \, dt$$

$$R_\mu = \frac{\langle \mu_1 \mu_2 \rangle}{\langle \mu^2 \rangle}$$

It is assumed that $x = 0$ at $t = 0$.

The calculation leading to Equation (7) is identical to the one given in Reference 5 for the Brownian motion of a particle with linear damping. Details of the calculation may be found in the next section, where the correlation function is obtained.

6

For large time, $t \gg \frac{1}{\beta}$, $\langle x^2 \rangle$ reaches a finite limit:

$$\langle x^2 \rangle = \epsilon^2 a_\infty^2 \frac{\tau_\mu}{\beta} \tag{8}$$

Because of this constant limit, x for large time may be treated as a stationary random function.

It is interesting to compare Equation (8) with the well known result for $\beta = 0$, corresponding to an unrestricted random walk:

$$\langle x^2 \rangle_{\beta=0} = 2 \epsilon^2 a_\infty^2 \tau_\mu t \tag{9}$$

Without the restoring mechanism, displacement continues to grow with time. The asymptotic value given by Equation (8) is also given by Equation (9) when $t = 1/2\beta$. If the restoring mechanism is thought of as limiting the time during which an unrestricted random walk takes place, then it is clear that β must be related to the integral time scale of the x motion. The integral time scale is found from the correlation function, which will now be calculated.

2.1.2 Correlation Function and Integral Scale — The correlation function $R_x(\tau)$ is defined as:

$$R_x(t_1, t_2) = \frac{\langle x(t_1) x(t_2) \rangle}{\langle x^2 \rangle} \tag{10}$$

x is assumed to be homogeneous and isotropic, so that

$$R_x(t_1, t_2) = R_x(t_1 - t_2) = R_x(t_2 - t_1) = R_x(\tau) \tag{11}$$

7

Working from Equation (5) and setting $\langle x(t_1) \; x(t_2) \rangle = \langle x \, x \rangle$,

$$\langle x \, x \rangle = e^{-\beta t_1} \; e^{-\beta t_2} \; \epsilon^2 a^2_\infty \int_0^{t_1} \int_0^{t_2} \langle \mu(\xi_1) \mu(\xi_2) \rangle \; e^{\beta(\xi_1 + \xi_2)} \; d\xi_1 \; d\xi_2 \qquad (12)$$

In view of Equation (11), take $t_1 = t$ and $t_2 = t + \tau$. Equation (12) becomes:

$$\langle x \, x \rangle = e^{-2\beta t} \; e^{-\beta \tau} \epsilon^2 a^2_\infty \int_0^t d\xi_1 \int_0^{t+\tau} d\xi_2 \; R_\mu(\xi_2 - \xi_1) \, e^{\beta(\xi_1 + \xi_2)} \qquad (13)$$

where $R_\mu(\xi_2 - \xi_1) = \langle \mu(\xi_1) \mu(\xi_2) \rangle$ (recall that $\langle \mu^2 \rangle = 1$). The form of Equation (13) suggests the obvious change of variable to center of mass and relative coordinates:

$$\xi_0 = \frac{\xi_1 + \xi_2}{2}$$

$$\xi = \xi_2 - \xi_1$$

$$(14)$$

The Jacobian $J = \dfrac{\partial(\xi_1 , \xi_2)}{\partial(\xi_0 , \xi)} = 1$ so that $d\xi_0 \, d\xi = d\xi_1 \, d\xi_2$.

The range of ξ is from $-t$ to $t + \tau$. If the ξ_0 integration is performed first, this range gives the integration limits for ξ, and the limits for ξ_0 become a function of ξ as well as t and τ. The limits on ξ_0 are seen with the aid of Figure 3, a sketch of the integration domain in $\{\xi_1 , \xi_2\}$ space. These limits are:

$$\xi \leq \tau , \qquad\qquad \frac{|\xi|}{2} \leq \xi_0 \leq t + \frac{\xi}{2}$$

$$(15)$$

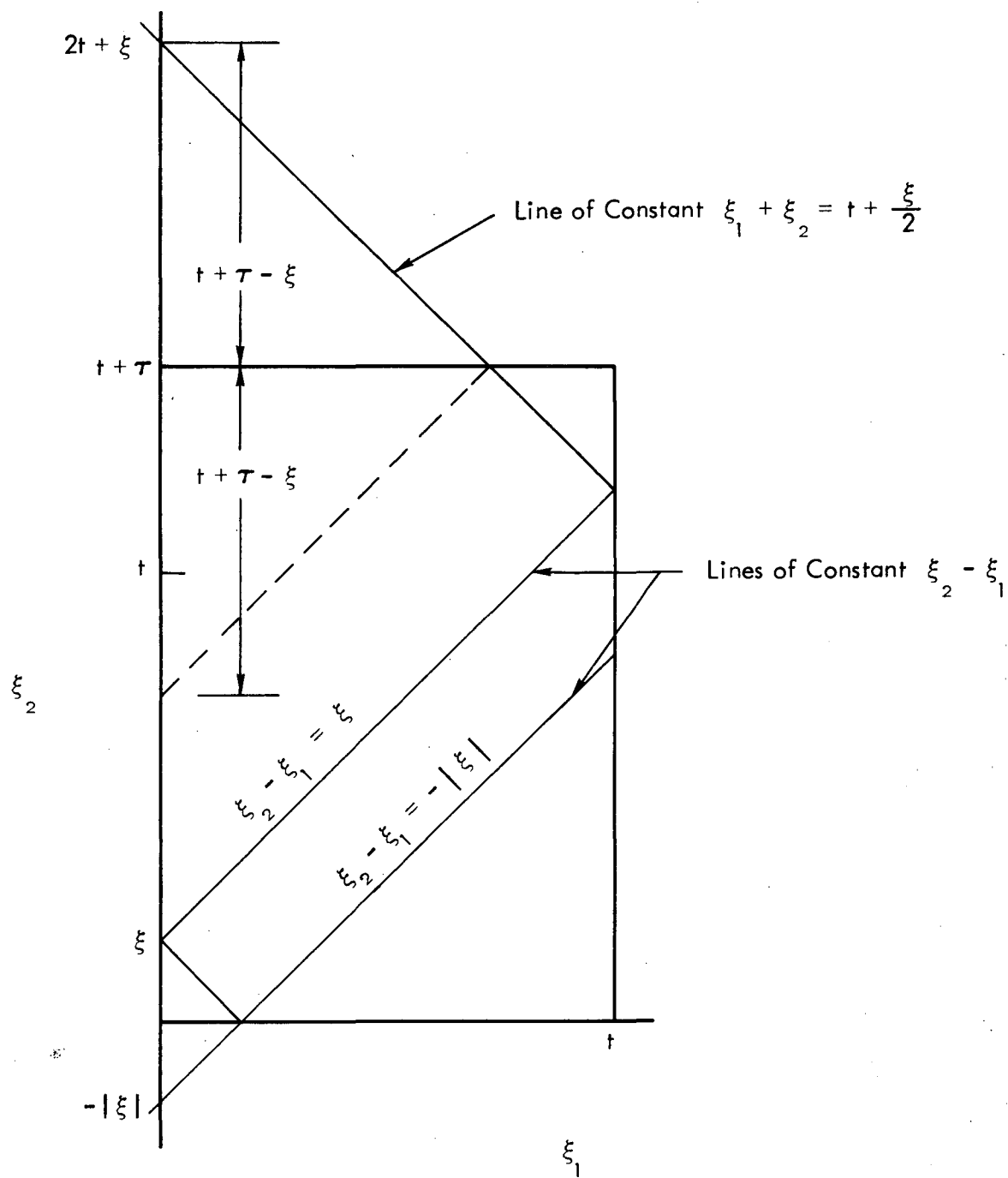$$\xi \geq \tau , \qquad\qquad \frac{|\xi|}{2} \leq \xi_0 \leq t + \tau - \frac{\xi}{2}$$

8

Figure 3. Domain of Integration

9

B

Equation (13) becomes:

$$\langle x\,x \rangle = e^{-2\beta t}\, e^{-\beta \tau}\, \epsilon^2\, a_\infty^2 \left\{ \int_{-t}^{\tau} d\xi \int_{\frac{|\xi|}{2}}^{t+\frac{\xi}{2}} d\xi_0 \, R_\mu(\xi)\, e^{-\beta \xi_0} + \right.$$

$$\left. + \int_{\tau}^{t+\tau} d\xi \int_{\frac{|\xi|}{2}}^{t+\tau-\frac{\xi}{2}} d\xi_0 \, R_\mu(\xi)\, e^{-2\beta \xi_0} \right\} \qquad (16)$$

or

$$\langle x\,x \rangle = e^{-2\beta t}\, e^{-\beta \tau}\, \epsilon^2\, a_\infty^2 \left\{ \int_{-t}^{\tau} d\xi \, R_\mu(\xi)\, I_1(\xi) + \int_{\tau}^{t+\tau} d\xi \, R_\mu(\xi)\, I_2(\xi) \right\} \qquad (17)$$

where

$$I_1 = \int_{\frac{|\xi|}{2}}^{t+\frac{\xi}{2}} e^{-2\beta \xi_0}\, d\xi_0 = \frac{e^{2\beta t}}{2\beta} \left[e^{\beta \xi} - e^{\beta |\xi|}\, e^{-2\beta t} \right]$$

$$(18)$$

$$I_2 = \int_{\frac{|\xi|}{2}}^{t+\tau-\frac{\xi}{2}} e^{-2\beta \xi_0}\, d\xi_0 = \frac{e^{2\beta t}}{2\beta} \left[e^{2\beta \tau}\, e^{-\beta \xi} - e^{\beta |\xi|}\, e^{-2\beta t} \right]$$

Using I_1 and I_2 in Equation (17) and re-arranging terms,

$$\langle xx \rangle = \frac{\epsilon^2 a_\infty^2}{2\beta} e^{-\beta T} \left\{ \int_{-t}^{T} e^{\beta \xi} R_\mu(\xi) \, d\xi + e^{2\beta T} \int_{T}^{t+T} e^{-\beta \xi} R_\mu(\xi) \, d\xi - \right.$$

$$\left. - e^{-2\beta t} \int_{-t}^{t+T} e^{\beta |\xi|} R_\mu(\xi) \, d\xi \right\} \tag{19}$$

Now, $R_\mu(\xi) \to 0$ for $\xi \gg \tau_\mu = \int_{0}^{\infty} R(\xi) \, d\xi$. (Note that ξ must simply be larger than several τ_μ for this condition to be satisfied.) If we assume that $R_\mu \to 0$ quickly enough so that $e^{\beta \xi} R_\mu(\xi) \to 0$, then for $t \gg \tau_\mu$ we may replace the limits $-t$ and $t+T$ by $-\infty$ and $+\infty$. Doing so, and taking the limit $t \to \infty$ so that the last term in Equation (19) vanishes,

$$\langle xx \rangle = \frac{\epsilon^2 a_\infty^2}{2\beta} e^{-\beta T} \left\{ \int_{-\infty}^{T} e^{\beta \xi} R_\mu(\xi) \, d\xi + e^{2\beta T} \int_{T}^{\infty} e^{-\beta \xi} R_\mu(\xi) \, d\xi \right\} \tag{20}$$

If $1/\beta \gg \tau_\mu$, then $e^{\beta \xi}$ and $e^{-\beta \xi}$ may be replaced by 1 in the integrals. Making this approximation, and re-arranging the integrals, we obtain:

$$\langle xx \rangle = \frac{\epsilon^2 a_\infty^2}{2\beta} \left\{ \left(e^{\beta T} + e^{-\beta T} \right) \int_{0}^{\infty} R_\mu(\xi) \, d\xi - \left(e^{\beta T} - e^{-\beta T} \right) \int_{0}^{T} R_\mu(\xi) \, d\xi \right\} \tag{21}$$

For $T \gg \tau_\mu$, the upper limit on the second integral may be changed to ∞. It is expected that $1/\beta \gg \tau_\mu$ (and this approximation has been made above), so that T will be larger than τ_μ over most of the range of the correlation function. This gives $\int_{0}^{\infty} R_\mu(\xi) \, d\xi = \tau_\mu$ for both integrals, so that the result for $T \gg \tau_\mu$ (again, this condition is just T larger than several τ_μ) is

11

$$\langle x x \rangle = \epsilon^2 a_\infty^2 \frac{\tau_\mu}{\beta} e^{-\beta\tau} \tag{22}$$

The correlation function is:

$$R_x(\tau) = \frac{\langle x x \rangle}{\langle x^2 \rangle} = e^{-\beta\tau} \tag{23}$$

The integral scale of x fluctuations is thus

$$\tau_x = \int_0^\infty e^{-\beta\tau} d\tau = \frac{1}{\beta} \tag{24}$$

This bears out the intuitive notion that β is closely related to the integral time scale of x fluctuations.

The mean square x excursion is given by using this in Equation (8):

$$\langle x^2 \rangle = \epsilon^2 a_\infty^2 \tau_\mu \tau_x \tag{25}$$

For $\tau < \tau_\mu$, Equations (22) through (25) are not valid. For $\tau < \tau_\mu$, $\beta\tau \ll 1$, so that $e^{\pm\beta\tau} \approx 1 \pm \beta\tau$. Equation (21) may be written:

$$\langle x x \rangle \approx \frac{\epsilon^2 a_\infty^2}{2\beta} \left\{ 2 \int_0^\infty R_\mu(\xi) d\xi - 2\beta\tau \int_0^\tau R_\mu(\xi) d\xi \right\} \tag{26}$$

For $\tau \ll \tau_\mu$, the second integral in Equation (26) is approximately τ. Thus

12

$$\langle x x \rangle \approx \frac{\epsilon^2 a_\infty^2}{\beta} \tau_\mu \left[1 - \frac{\beta}{\tau_\mu} \tau^2 \right] \qquad (27)$$

for small τ. This result will be used later in discussing the predicted spectrum.

2.1.3 Pressure Flucutations — If the pressure due to the shock wave at its mean location is $P(\bar{x})$, then the pressure at time t is given by $P(\bar{x} - x(t))$. The fluctuating pressure from shock oscillation is then

$$p(\bar{x}, t) = P(\bar{x} - x(t)) - P(\bar{x}) \qquad (28)$$

where $\bar{x}$ denotes the streamwise coordinate and $x(t)$ is the excursion. The mean square pressure fluctuation is:

$$\langle p^2 \rangle = \langle [P(\bar{x} - x(t)) - P(\bar{x})]^2 \rangle \qquad (29)$$

If ξ is small, $P(\bar{x} - x)$ may be expanded in a Taylor series:

$$\langle p^2 \rangle = \langle [P(\bar{x}) - x(t) P'(\bar{x}) + \dots - P(\bar{x})]^2 \rangle \qquad (30)$$

so that for $\xi \ll \frac{P}{P'}$

$$\langle p^2 \rangle = \langle [\xi(t) P'(\bar{x})]^2 \rangle = [P'(\bar{x})]^2 \langle x^2 \rangle \qquad (31)$$

This is accurate only when $\langle x^2 \rangle^{\frac{1}{2}}$ is small compared to shock thickness. If $\langle x^2 \rangle^{\frac{1}{2}}$ is not small, Equation (29) would have to be used. This would require the probability distribution function of x, which has not been calculated.

13

2.1.4 Spectral Density — The spectral density of the mean square pressure fluctuations is defined as the Fourier transform of the correlation function:

$$\phi(f) = 4\langle p^2 \rangle \int_0^\infty R_p(\tau) \cos 2\pi f \, d\tau \qquad (32)$$

where the factor $4\langle p^2 \rangle$ appears so that $\int_0^\infty \phi(f) \, df = \langle p^2 \rangle$. This definition of ϕ is consistent with the notation of Reference 1.

Assuming that $\langle x^2 \rangle$ is small enough so that Equation (31) is valid, $R_p(\tau) = R_x(\tau)$. Using Equation (23) in Equation (32), it is straightforward to obtain

$$\phi(f) = \frac{4\langle p^2 \rangle}{\beta \left[1 + \left(\dfrac{2\pi f}{\beta} \right)^2 \right]} \qquad (33)$$

Because Equation (23) is not accurate for $\tau < \tau_\mu$, Equation (33) is not accurate for $f > \dfrac{1}{2\pi \tau_\mu}$. For $f \gg \dfrac{1}{2\pi \tau_\mu}$, $\phi(f)$ is given by the transform of Equation (27). This behaves asymptotically as f^{-3}, compared to f^{-2} for Equation (33). Equation (33), then will tend to be too large at high frequencies $f > \dfrac{1}{2\pi \tau_\mu}$.

2.2 Prediction of Pressure Fluctuations Ahead of a 45° Wedge

The fluctuating pressure intensity and spectra are given by Equations (31) and (33), with Equation (8) giving $\langle x^2 \rangle$ and Equation (24) relating τ_x to β. Given the mean flow conditions, the parameters required are the boundary layer turbulent intensity ϵ and integral scale τ_μ, and the integral scale τ_x of the shock motion.

Predictions will now be made for the 8 inch, 45° wedge of Reference 2. This particular set of measurements is chosen because the two-dimensional geometry is simple, and because of the good quality of both fluctuating and mean measurements.

14

2.2.1 Flow Parameters — The following are the mean flow parameters required:

$$M_\infty = 2.0$$

$$\delta_0 = 4 \text{ inches}$$

$$h = 8 \text{ inches}$$

The pressure gradient at the mean shock location is required. Figure 4 gives the mean pressure coefficient and root mean square fluctuating pressure for several test models in Reference 2. Measuring the slope for the 45° wedge case at the mean shock location,

$$P'(0) = 0.42 \frac{q_\infty}{h} = 0.21 \frac{q_\infty}{\delta_0} \tag{34}$$

From Equation (32), the integral scale is given by:

$$\tau_i = \int_0^\infty R_i(\tau) \, d\tau = \frac{1}{4} \frac{\phi_i(0)}{\langle p^2 \rangle} \tag{35}$$

where i is μ or x. The integral scales are easily found from the 0 frequency point in Figure 2, and are

$$\tau_x = 25 \frac{\delta_0}{u_0}$$

$$\tag{36}$$

$$\tau_\mu = 1.9 \frac{\delta_0}{u_0}$$

From Figure 4, $\langle p^2 \rangle^{\frac{1}{2}} / q_\infty = 0.003$ for the boundary layer. Turbulent velocity fluctuations are related to pressure fluctuations by (Reference 6):

$$\langle p^2 \rangle^{\frac{1}{2}} = 0.7 \, \rho \, \langle u^2 \rangle = 0.7 \, \rho \, \epsilon^2 \, a_\infty^2 \tag{37}$$
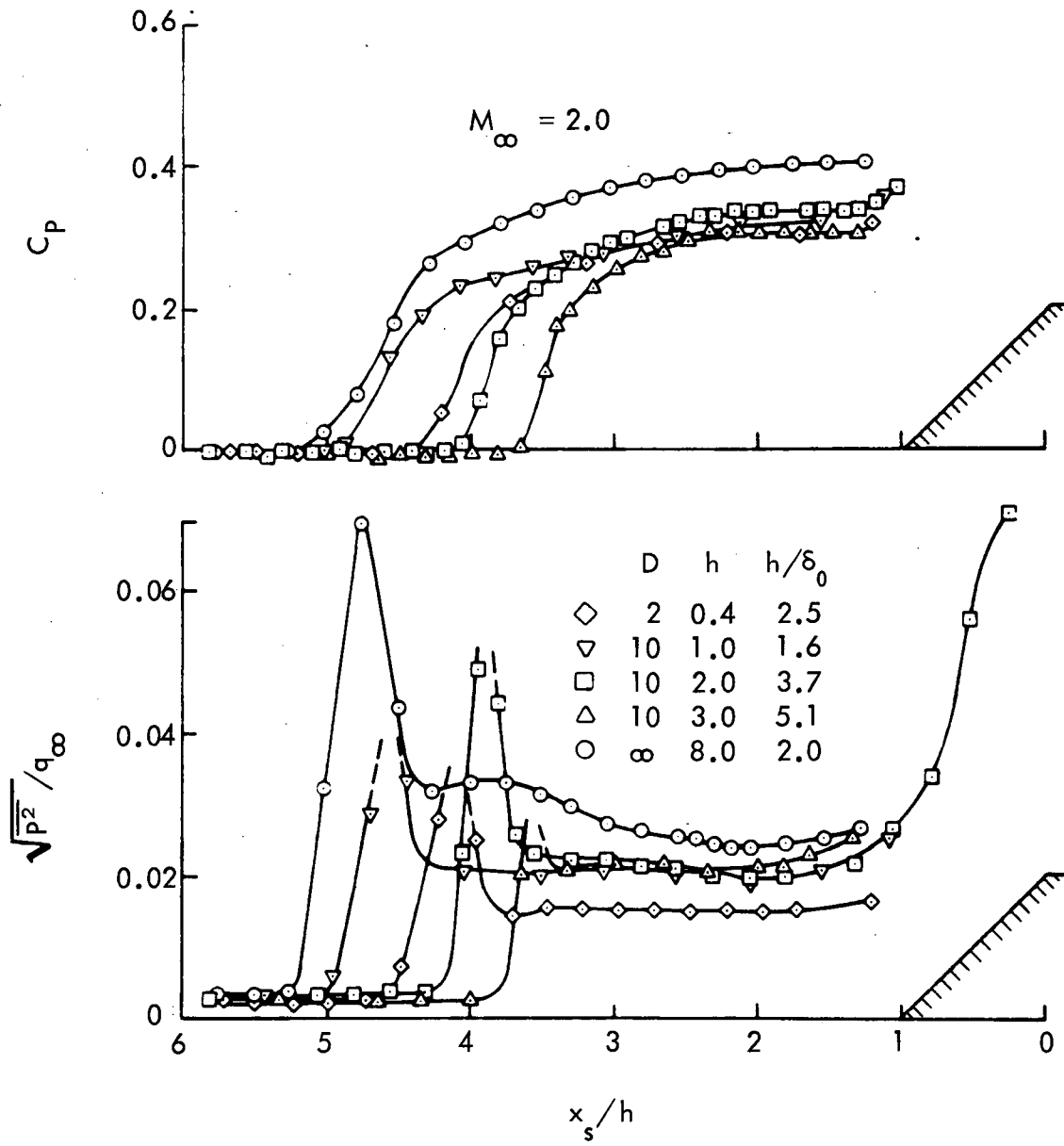
15

Figure 4. Longitudinal Distributions of Steady and Fluctuating
Pressures, from Reference 2

16

Taking $\rho = \rho_\infty$,

$$\epsilon^2 = \frac{M_\infty^2}{1.4} \frac{\langle p^2 \rangle^{\frac{1}{2}}}{q_\infty} \tag{38}$$

Using $\langle p^2 \rangle^{\frac{1}{2}} = 0.003\, q_\infty$,

$$\epsilon^2 = 0.00214\, M_\infty^2 \tag{39}$$

All required parameters have now been obtained.

2.2.2 Root Mean Square Pressure Fluctuations — Using the above values in Equation (8),

$$\langle x^2 \rangle = \epsilon^2 a_\infty^2\, \tau_\mu\, \tau_x$$

$$= 0.00214\ M_\infty^2\ a_\infty^2 \cdot 25\, \frac{\delta_0}{u_0} \cdot 1.9\, \frac{\delta_0}{u_0}$$

$$= 0.102\ \delta_0^2$$

so that the root mean square displacement is

$$\langle x^2 \rangle^{\frac{1}{2}} = 0.32\, \delta_0 \tag{40}$$

This is smaller than the shock thickness (which is of order δ_0), so that Equation (31) may be used for the pressure. The fluctuation at the mean shock location is

17

$$\langle p^2 \rangle^{\frac{1}{2}} = P'(0) \langle x^2 \rangle^{\frac{1}{2}} = 0.214 \frac{q_\infty}{\delta_0} \cdot 0.32 \, \delta_0$$

$$\frac{\langle p^2 \rangle^{\frac{1}{2}}}{q_\infty} = 0.68 \tag{41}$$

This is in excellent agreement with the value of 0.7 in Figure 4.

2.2.3 Spectrum — Figure 5 shows the predicted spectrum, Equation (33), along with the shock spectrum from Figure 2 and two spectra measured by Robertson (Reference 1) for three—dimensional protuberances. Except for being slightly high at higher frequencies, the agreement is excellent. $f\delta/u = 10^{-1}$ corresponds approximately to $f = \frac{1}{2\pi\tau_\mu}$, where Equation (33) is not expected to be accurate. The slope of the measured spectra at this point corresponds to $f^{-2.6}$, which is between the f^{-2} behavior of Equation (33) and the f^{-3} behavior of the high frequency limit discussed in Section 2.1.4. A spectrum calculated from Equation (21) would show even better agreement with the data.

Above $f\delta_0/u_\infty \approx 2 \cdot 10^{-1}$, the measured spectrum is dominated by separated flow fluctuations, as pointed out by Robertson (Reference 1), and the present analysis does not apply.
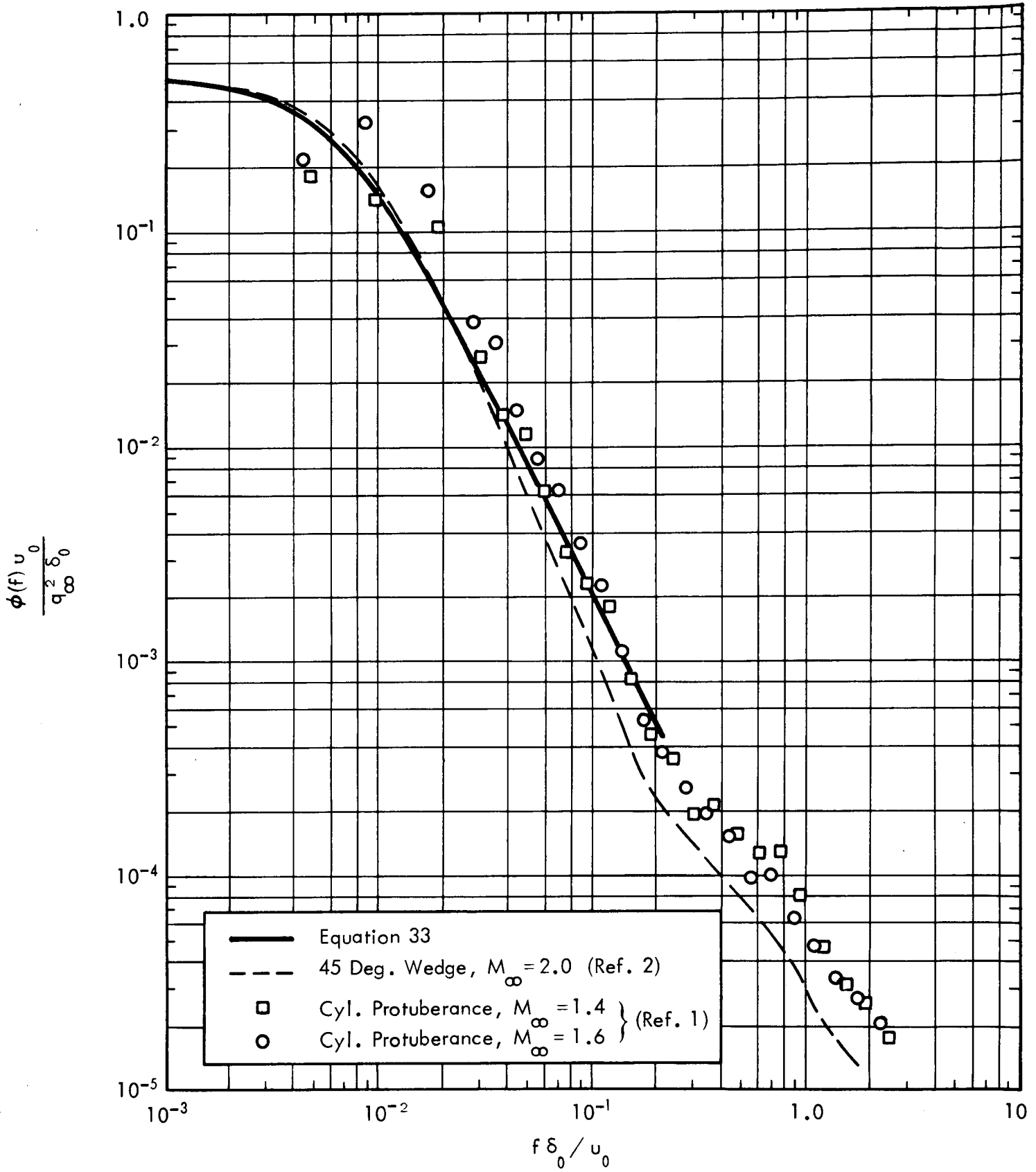
Figure 5. Comparison of Predicted Spectrum with Measured Spectra

3.0 CONCLUSIONS

A simple mechanism has been proposed for the pressure fluctuations near a shock wave interacting with a turbulent boundary layer. The shock wave is convected from its mean location by velocity fluctuations in the turbulent boundary layer, while stability of the mean flow tends to restore the shock wave to its original position. The restoring mechanism is assumed to be linear. The motion of the shock wave, given by Equation (5), is quite similar to the Brownian motion of a particle. The mean square displacement tends to a constant value at large time, given by Equation (8), so that the motion may be treated as a stationary random function. The mean square pressure fluctuation, Equation (31), and spectral density, Equation (33), calculated from this shock motion are in excellent agreement with experimental data.

Because of the excellent agreement of the present theory with experimental data, and the straightforward physical model employed, it is concluded that turbulent boundary layer fluctuations are the dominant cause of shock wave oscillation in the case of flare and protuberance induced separated flow.

REFERENCES

1. Robertson, J.E., "Prediction of In-Flight Fluctuating Pressure Environments Including Protuberance Induced Flow," Wyle Laboratories Research Staff Report WR 71-10, March 1971.

2. Coe, C.F., and Rechtien, R.D., "Scaling and Spatial Correlation of Surface Pressure Fluctuations in Separated Flow at Supersonic Mach Numbers," Paper presented at the AIAA Structural Dynamics and Aeroelasticity Specialist Conference, New Orleans, Louisiana, April 16-17, 1969.

3. Trilling, Leon, "Oscillating Shock-Boundary Layer Interaction," J. Aero. Sci., 25, No. 5, 1958.

4. Karashima, K., "Instability of Shock Wave on Thin Airfoil in High Subsonic Flow," Aeronautical Research Institute, University of Tokyo, Report No. 363, March 1961.

5. Uhlenbeck, G.E., and Ornstein, L.S., "On the Theory of Brownian Motion," Phys. Rev., 36, No. 3, Sept. 1930. Reprinted in Selected Papers on Noise and Stochastic Processes, edited by Nelson Wax, Dover, New York, 1954.

6. Hinze, J.O., Turbulence , McGraw-Hill, 1959, Section 3-8.